Journal of Catalysis 366 (2018) 37–49

Contents lists available at ScienceDirect

Journal of Catalysis

journal homepage: www.elsevier.com/locate/jcat

Direct ring C—H bond activation to produce cresols from toluene and hydrogen peroxide catalyzed by framework titanium in TS-1

Conglin Pang, Jiahui Xiong, Guiying Li *, Changwei Hu *

Key Laboratory of Green Chemistry and Technology, Ministry of Education, College of Chemistry, Sichuan University, Chengdu, Sichuan 610064, PR China

ARTICLE INFO

Article history:
Received 21 June 2018
Revised 28 July 2018
Accepted 30 July 2018

Keywords:
Toluene
Cresols
TS-1
Hydrogen peroxide
Ring-oxidation
Framework Ti

ABSTRACT

A series of TS-1 samples with varying Ti content was prepared and applied in the partial oxidation of toluene with H_2O_2 as oxidant. The TS-1 samples and relevant systems were characterized by XRD, FT-IR, *in situ* FT-IR, nitrogen adsorption/desorption, DR UV–vis, XPS, ICP-AES, EPR, SEM, TEM and TG. The results showed that the framework Ti species was responsible for the selective ring C—H bond activation, resulting in toluene hydroxylation; while the extra-framework Ti species was advantageous to the formation of side chain oxidation products and to the deep oxidation of both kinds of the products formed. Under the optimized reaction conditions, the toluene conversion reached 38.9% with 84.3% selectivity to cresols (TOF, 2.66 h^{-1}), while, the selectivity of para-cresol was 66.8%, which might be caused by the pore structure and steric hindrance of methyl group. The catalyst regenerated by calcination exhibited stable activity and selectivity after the second run.

1. Introduction

Selective oxidation of aromatic carbon-hydrogen (C—H) bonds to form new C—C, C—O, C—N bonds by one step process has attracted considerable attention for its wide application in industry [1,2]. The investigation of the direct hydroxylation of arenes with hydrogen peroxide under mild condition is mostly concentrated to the preparation of phenol from benzene [3,4]. However, substituted benzene is quite different and interesting, because of the challenge for getting high selectivity from competitive reactions existed between ring sp^2 C—H bond activation and side chain sp^3 C—H activation [5,6], among them, ring C—H bond activation is usually expected. Meanwhile, thanks to the directing groups, the control of the region-selectivity in C—H activation was worth discussing [7].

Titanium silicalite-1 (TS-1) has received much attention and found large potential application during the last decade for its excellent catalytic activity in selective oxidation of organics using aqueous H_2O_2 (30 wt%) as oxidant [8–10]. Typical reactions include the oxidation of alkanes and alcohols [11], aromatic hydroxylation [12–18], alkene epoxidation [19–22], as well as ketone ammoximation, etc [23,24]. It is well known that as the active component in TS-1, titanium plays an important role for the catalytic performance. However, two types of Ti species exist in TS-1 zeolite, that is, the [TiO_4] species tetrahedrally coordinated in the framework [25–29], and the octahedral anatase-like TiO_2 species or amorphous Ti species in the extra-framework [27,30]. Therefore, it is of paramount importance to study the influence of these two kinds of titanium species on the reaction. Guang et al. [20] found that among the two species, the framework Ti species was the active center for selective oxidation of propylene. Feng et al. [31] also thought that only isolated framework Ti(IV) species were responsible for the selective propene epoxidation with H_2 and O_2. Xia et al. [32] noted that the framework Ti was the active sites for phenol oxidation reaction, while the extra-framework Ti was unfavorable for the reaction because of unwanted promotion of the decomposition of H_2O_2.

Cresols are important intermediates for fine chemicals, which are widely employed for preparing phenolic resins, insecticides, herbicides and dyes [33–35]. Generally, worldwide industrial production of cresols was carried out from toluene *via* a multistep reaction processes including sulfonated alkali fusion [36], chlorination [35] or cymene process [33]. The multistep processes have many disadvantages, such as, energy and time consuming with harsh operation conditions, low atom efficiency, large amount of by-products and serious environmental pollution [35,37]. Studies on the hydroxylation of aromatic compounds with various metal-modified catalysts have been reported in literatures [17,26,38]. The catalysts investigated in the direct oxidation of toluene are

* Corresponding authors.
E-mail addresses: gchem@scu.edu.cn (G. Li), changweihu@scu.edu.cn (C. Hu).

https://doi.org/10.1016/j.jcat.2018.07.038
0021-9517/

mostly porous zeolite materials, such as SBA-15 [39–41], ZSM-5 [42–44], MCM-41 [45–47], activated carbon (AC) [48] and so on. On this basis, the materials were usually modified by various transition metals such as Ti [45], Pt [39], Fe [48] and so on. Nevertheless, most of the products are side chain oxidation products. The conventional impregnation method has the problems of energy consuming and the catalysts obtained suffer from metal's leaching, which limited their application [49]. Among them, titanium-modified materials (i.e, TS-1) have inestimable advantages, for the Ti species predominantly in tetrahedral co-ordination could be obtained by direct hydrothermal synthesis, getting rid of metal leaching [50].

At present, some literatures on the influence of different titanium environments in TS-1 catalyst for hydroxylation of aromatics have been reported. Barbera et al. [4] evaluated the different titanium species by UV–vis and IR spectroscopy, and reported that the extra-framework Ti species did not contribute to benzene hydroxylation. Luo et al. [3] described a TS-1 without extra-framework Ti and got an excellent phenol yield of 39% with 72% selectivity. Comparative study on the commercial TS-1 bearing both framework Ti and extra-framework Ti, showed that framework Ti species were responsible for the direct hydroxylation of benzene to phenol, while the extra-framework TiO_2 species caused decrease of activity. However, the hydroxylation of toluene for ring C—H activation was studied rarely in literatures [33]. Liu et al. prepared TS-1/diatomite catalyst, which was treated with H_2SO_4/HF mixed acid solution and calcined at 1000 °C, and then used for toluene hydroxylation by H_2O_2 with acetone solvent in fixed-bed reactor. This reaction got a high cresol selectivity of 97.1% with the 14.3% conversion of toluene.

However, some challenges still remains, for example, what kind of titanium species playing a pivotal role in the hydroxylation of substituted benzene such as toluene has not been reported. Thus, in this work, various TS-1 samples were synthesized with different Ti content, and applied for toluene partial oxidation. The roles of different Ti species on toluene hydroxylation were researched, and the reaction conditions for the hydroxylation of toluene were optimized.

2. Experiment

2.1. Catalyst preparation

The TS-1 samples were synthesized following the procedures reported in the literatures [12], which was a modified one of that reported in Ref. [51]. The molar compositions of the components were the following: 1.0 SiO_2: 0.36TPAOH: xTiO_2: 27H_2O, among them, TEOS (tetraethyl orthosilicate, 98%) and $TiCl_3$ (titanium trichloride, 15–20%) was used as SiO_2 and TiO_2 source, respectively. The mixture was heated at 55 °C for 1 h and 85 °C for 8 h with continuous dripping of water to ensure the total volume invariant. The resulted solution was cooled down to room temperature and kept standing for about 12 h. After that, the mixed liquid was aged at 175 °C for 7 days in a 0.3 L autoclave under autogeneous pressure. The crystallized solid was filtered, washed and dried at 110 °C. Finally the sample was calcined at 550 °C for 10 h and the TS-1 catalyst was obtained. The TS-1 with various controlled Ti contents were denoted as TS-1a (x = 0, silicate-1), TS-1b (x = 0.89%), TS-1c (x = 1.48%), TS-1d (x = 2.96%) and TS-1e (x = 5.92%).

The calcined TS-1a (S-1) sample was crushed and sieved, then the particles were dipped in aqueous solution of active ingredient $TiCl_3$ (the molar ratio of titanium to silicon was the same as TS-1e), then dried at 80 °C to remove the solvent, calcined at 550 °C to get the Ti/S-1 catalyst.

The TiO_2 sample (>99.0% CAS13463-67-7) was commercially obtained from Kelong Chemical Reagent Factory, Chengdu, China.

2.2. Characterization

2.2.1. X-ray diffraction (XRD)

XRD analyses of both fresh and used catalysts were carried out on an LED DX-1000 CSC Diffractometer with a Cu Kα monochromatic X-ray radiation (λ = 0.15406 nm), and the data were collected over the 2Θ range of 5° to 35° with a step of 0.06°/min.

2.2.2. Fourier transform infrared spectroscopy (FT-IR)

Samples were diluted with KBr and pressed. The FT-IR data were collected on a VERTEX 70 FT-IR spetrometer equipped with an MCT detector in the region of 4000–400 cm^{-1} with a resolution of 4 cm^{-1}.

In situ FT-IR spectra of the deactivated TS-1 catalyst were carried out on a FT-IR spectrometer (Bruker VERTEX 70) with a MCT detector cooled by liquid nitrogen. The instrument could obtain the information over the frequency range of 4000–900 cm^{-1}, and the spectra resolution was 4 cm^{-1}. Prior to the experiment, the sample (about 20 mg) was pretreated at 100 °C under vacuum for 1 h to avoid the moisture. The background spectrum was collected from 20 to 500 °C at a rate of 10°/min under Ar flowing rate of 30 mL/min, and the spectral acquisition was performed at the same heating rate in a dry air atmosphere. The final spectra were obtained by subtracting the spectrum at the same temperature points in Ar flow.

2.2.3. Nitrogen adsorption/desorption

The Brunauer-Emmett-Teller (BET) surface area (S_{BET}), the single point adsorption total pore volume of pores (V_{total}), t-Plot micropore volume (V_{mic}), mesopore volume (V_{meso}) and the average pore diameter (D_{avg}) of the catalysts were measured at −196 °C on a Micromeritics Tristar 3020 instrument. Peior to N_2 physisorption, 0.10 g catalyst was pretreated at 150 °C for 2 h and 300 °C for 2 h under vacuum.

2.2.4. Ultraviolet–visible diffuse reflectance (DR UV–vis)

The DR UV–vis spectra were examined by a TU-1901 spectrometer at the scan range from 200 to 800 nm with $BaSO_4$ as the reference sample. All the UV–vis patterns of TS-1 were processed by the software of Peakfit v4.12.

2.2.5. X-ray photoelectron spectroscopy (XPS)

XPS was used to provide information on the surface composition of the TS-1 with different Ti content, and it was performed with an AXIS Ulttra DLD (KRATOS) spectrometer equipped with a monochromatic Al-Kα x-ray source (excitation energy = 1486.6 eV). Spectrum curve fitting was carried out using the Casa XPS software.

2.2.6. Scanning electron microscopy (SEM)

The morphologies of all the catalysts were examined by SEM (JSM-7500F, JEOL, Tokyo, Japan) with energy dispersive spectroscopy (EDX). The voltage was set at 5 KV. A thin film of gold was applied to improve the conductivity of the samples.

2.2.7. Transmission electron microscopy (TEM)

TEM measurements of the TS-1 catalysts were carried out on JEOL JEM-2100 electron microscope equipped with a field emission source working at 200 KV.

2.2.8. Inductively coupled plasma-atomic emission spectrometry (ICP-AES)

The catalyst samples were dissolved in HF solution in a Teflon vessel for about 12 h, then the HF was evaporated and the solid was dissolved in aqua regia to prepare samples for ICP-AES. The ICP-AES measurement was performed to determine the actual Ti

content on a VGPQExCell instrument (TIA, Boston, MA, USA). The Ti content of fresh and spent TS-1 samples from ICP analyses were listed in Tables 2 and 4, respectively.

2.2.9. Thermo-gravimetric Analysis (TG)

TG was used to analyze the deposited carbon of the used catalysts on a Thermo-gravimetric analysis apparatus (TG, NETZSCH TG 209F1). Approximately 10 mg sample was heated from 30 °C to 800 °C with the rate of 10 °C/min in dry air under the flowing rate of 60 mL/min.

2.2.10. Electron Paramagnetic Resonance (EPR)

EPR spectra were recorded at ambient temperature on a Bruker EMX plus spectrometer to probe the radical species formed in this reaction system, the instrument parameters were as follows: microwave frequency 9.87 GHz, microwave power 10 mW, modulation frequency 100 kHz, scan time 2 min.

2.3. Catalyst activity test

The partial oxidation of toluene was carried out in a single necked flask reactor (50 mL) with reflux condenser at atmospheric pressure in open air. In a typical run, designed amount of catalyst, H_2O, hydrogen peroxide (30 wt%) and toluene were loaded in the flask in turn. Then the reaction was carried out with stirring when the temperature of the reactor reached a constant. When the designed reaction time was reached, the reaction was stopped immediately and cooled down to room temperature. At last, the products were qualitatively analyzed by GC-MS (Aglient, 5973 Nework6890N) and were quantified by HPLC (Aglient 1200) equipped with a ZORBAX Eclipse XDB-C18 column and an UV detector.

The yield and the selectivity of the products were calculated, ignoring the polymerization products, ring-opening products and tar, meanwhile the loss of volatility was taken into account in the calculation [36,37]:

$$\text{Yield}(\%) = \frac{moles\ of\ products\ (cresols, etc.)\ produced}{moles\ of\ initial\ toluene} \times 100;$$

$$\text{Selectivity of cresols}(\%) = \frac{moles\ of\ cresols\ produced}{moles\ of\ all\ products} \times 100;$$

$$\text{Conversion of } H_2O_2(\%) = \frac{moles\ of\ consumed\ H_2O_2}{moles\ of\ initial\ H_2O_2} \times 100;$$

$$\text{Selectiviry of } H_2O_2(\%) = \frac{moles\ of\ toluene \times [(Y_{cresols} + Y_{BM}) + 3 \times (Y_{HA} + Y_{MQ})]}{moles\ of\ initial\ H_2O_2 \times CH_2O_2} \times 100;$$

$$\text{TOF}\ \left(h^{-1}\right) = \frac{moles\ of\ cresols\ produced}{moles\ of\ total\ Ti \times reaction\ time}.$$

3. Results and discussion

3.1. Catalyst characterization

3.1.1. N_2 adsorption-desorption isotherms

Fig. 1 displayed the N_2 adsorption-desorption characterization of the prepared TS-1 samples, which was basically characteristic of TS-1 according to literature [52]. The controlled and actual Ti/Si molar ratio corresponding to different TS-1 samples were listed in Table 1, and their corresponding actual Ti contents (wt %) were listed in Table 2. In the following description, all of the Ti/Si molar ratio was referred to the actual Ti/Si molar ratio determined by ICP-AES analysis. As shown in Table 1, when the actual Ti/Si molar ratio on TS-1 was increased from 0 to 7.66%, the S_{BET} first increased until a maximum appeared for TS-1c (Ti/Si molar ratio = 1.75%), then decreased with further increase of Ti concentration. The value of total pore volume did not change with the increase of Ti/Si molar ratio from 0 to 1.75%, and then decreased remarkably with Ti/Si molar ratio from 1.75% to 7.66%, while the pore size decreased monotonically with increasing titanium content. The pore size distribution curves showed that the pore size of the TS-1 samples were concentrated at 15–25 Å, which was characteristic for mesoporous materials. In addition, the pore size distribution tended to shift to lower value with increasing titanium content. Contrary to the tendency of pore size variation, the V_{mic} gradually increased with the increase of titanium content. For the Nitrogen adsorption/desorption isotherms, TS-1d and TS-1e showed almost no difference between adsorption and desorption isotherms, which was consistent with type II isotherms. However, for samples with low titanium content, TS-1a, b and c, the type IV isotherms with H1 type hysteresis loop from $P/P_0 = 0.9$ to 1.0 appeared, which suggested a peculiar feature of mesoporous structure [53]. The results were probably caused by the fact that moderate Ti might enter the framework replacing the Si to make the molecular sieve structure more regular, while excessive titanium might present as extra-framework coated on the wall of the pores or cause meso-pore blocking effect [54]. It was interesting to note that mesopores

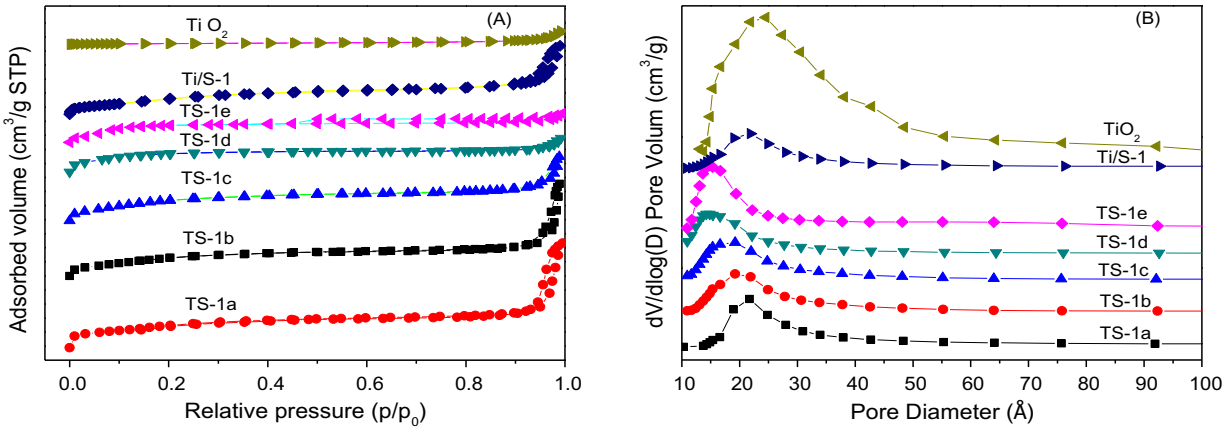

Fig. 1. (A) N_2 adsorption-desorption isotherms of the samples; (B) The pore diameter distribution of the samples.

Table 1
Physicochemical properties of the samples.

Sample	Ti/Si (%)[a]	Ti/Si (%)[b]	S_{BET} (m^2/g)	V_{total} (cm^3/g)	V_{mic} (cm^3/g)	V_{meso} (cm^3/g)	D_{avg} (Å)
TS-1a	–	–	383.04	0.36	0.13	0.23	27.29
TS-1b	0.89	1.05	419.55	0.35	0.14	0.21	25.24
TS-1c	1.48	1.75	463.54	0.34	0.16	0.18	23.11
TS-1d	2.96	3.62	399.48	0.24	0.16	0.08	20.19
TS-1e	5.92	7.66	388.18	0.25	0.17	0.08	19.62
Ti/S-1	5.92	ND	399.68	0.32	0.13	0.19	31.79
TiO_2	ND	ND	10.65	0.04	–	0.04	47.79

ND: not determined.
[a] The controlled molar ratio (%) in the preparation experiment above.
[b] The actual Ti/Si molar ratio (%) determined by ICP-AES analysis.

Table 2
The elemental analysis results of TS-1 samples with different Ti content.

Samples	ICP Ti_{total} (wt %)	XPS Ti_{total} (wt %)	I_{960}/I_{800} (FT-IR)	$Ti_{framework}/Ti_{total}$ (XPS)
TS-1a	–	–	–	–
TS-1b	0.83	0.10	0.10	1.00
TS-1c	1.36	0.19	0.19	1.00
TS-1d	2.75	0.44	0.20	0.45
TS-1e	5.54	0.53	0.18	0.34

volume (0.23 cm^3/g) was observed for silicalite sample (TS-1a) in comparison with the other samples, which might be caused by extra-framework amorphous materials [55]. It could be speculated that TS-1a might contain amorphous silica.

3.1.2. XRD

The XRD patterns of the catalysts with different Ti contents were plotted in Fig. 2. The formation of TS-1 with MFI (Zeolite Socony Mobil Five) structure was confirmed by the XRD characteristic patterns, indicated by the peaks at 2Θ of 7.9°, 8.8°, 23.1°, 23.9°, 24.4° [31,56]. The insertion of Ti in the framework of S-1 was indicated by the variation in Fig. 2 of the shape and size of the peak at 24.4 2Θ degree of sample TS-1a in comparison with the others [57].

3.1.3. FT-IR

The FT-IR absorption spectra of TS-1 samples were shown in Fig. 3(A). The TS-1 samples exhibited all the feature signals (i.e. 1225, 1100, 960, 800, 550 and 450 cm^{-1}) of the MFI type zeolite structure, which was consistent with the XRD results. Among them, a silanol group (Si—OH) peak at 930–970 cm^{-1} could be found for TS-1a, which indicated the presence of extra-framework amorphous silica [58–60]. Combining the mesoporosity in Table 1, we could conclude that silicalite-1 also contained extra-framework Si species. The peak at 960 cm^{-1} for TS-1b, c, d and e was ascribed to the interaction between the stretching vibration of [SiO_4] units [61] and titanium ions in neighboring coordination sites, which was an evidence of the vibration of Si—O—Ti bond in the framework [17,19,62]. The peak at 800 cm^{-1} was ascribed to the symmetrical stretching vibration of Si—O—Si bond in [SiO_4] [31,58]. The level of incorporation of Ti(IV) into the framework was usually calculated by the band intensity ratio of I_{960}/I_{800}. The higher the ratio, the more was the amount of framework Ti. The ratio in Fig. 3(B). and Table 2 showed that the amount of framework Ti had the following order TS-1a < TS-1b < TS-1c ≈ TS-1d ≈ TS-1e. It could be observed that the amount of titanium

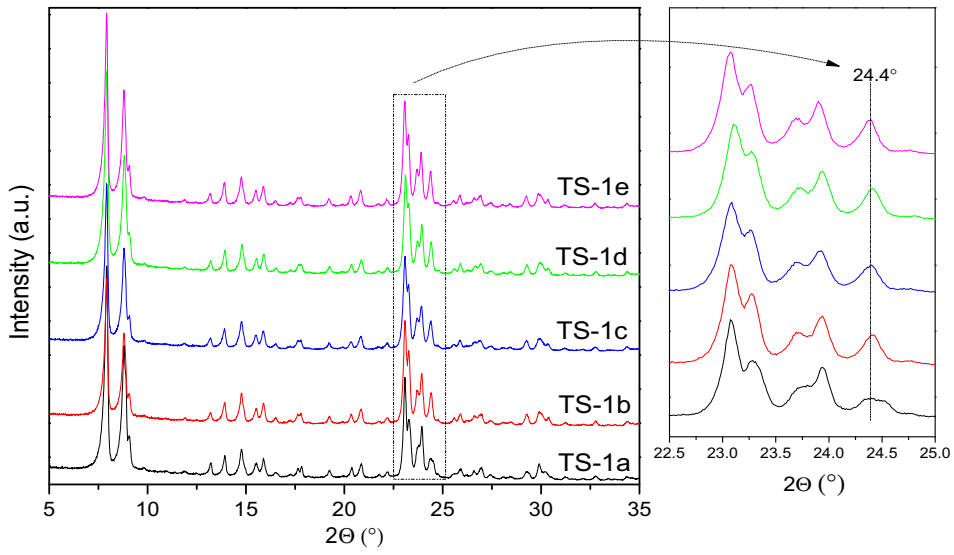

Fig. 2. XRD patterns of TS-1 samples with different Ti content.

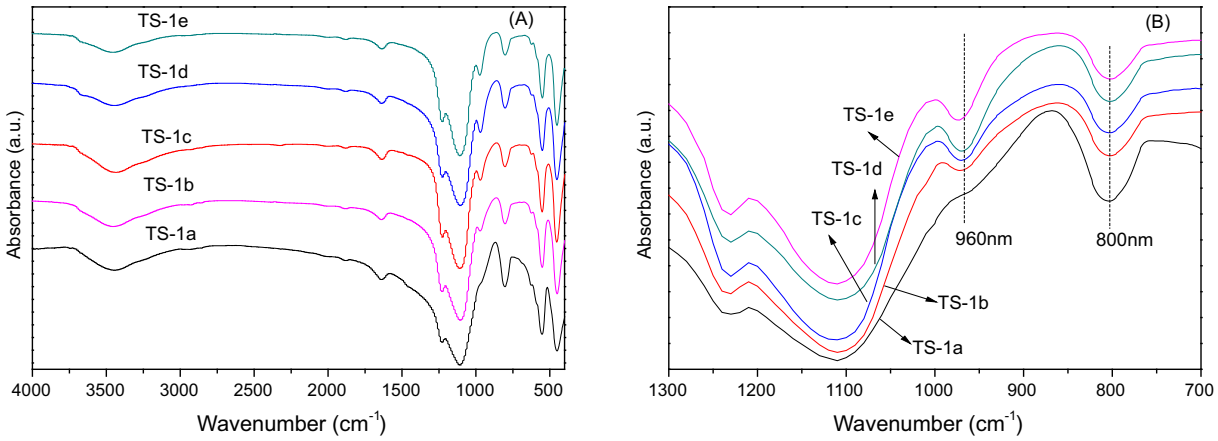

Fig. 3. The FT-IR spectra of TS-1 samples with different Ti content.

incorporated into the silicon framework has a threshold, over which the excess titanium could not incorporate into the framework, but existed as extra-framework titanium species. This result again demonstrated that the decrease in S_{BET}, V_{total} and D_{avg} in the BET characterization was resulted from the formation of extra-framework titanium species.

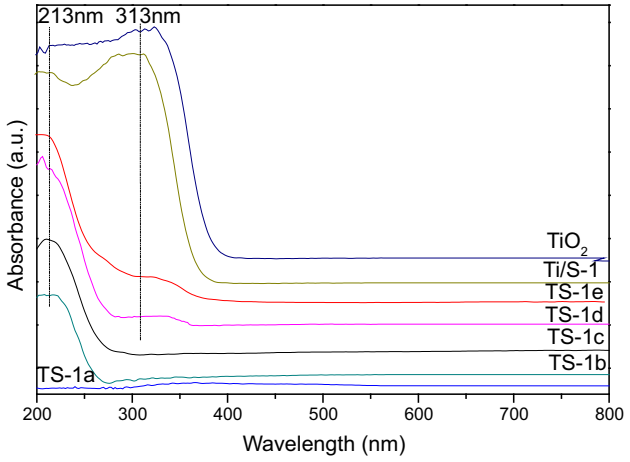

Fig. 4. The DR UV–vis spectra of the samples.

3.1.4. DR UV–vis

Fig. 4 showed the UV–vis spectroscopy of TS-1 with different Ti content. TS-1a did not exhibit any characteristic spectra because no Ti was added. The bands at 213 nm and 313 nm corresponded to framework Ti and extra-framework Ti respectively [32]. On TS-1b and TS-1c, the bands around 213 nm, originated from Ti^{4+}-$O^{2-} \rightarrow Ti^{3+}O^{-}$ of framework tetrahedral [TiO_4] species, was observed [63]. While for TS-1d and TS-1e, in addition to the peak at 213 nm, a new peak appeared above 300 nm, which was attributed to extra-framework TiO_2 [63]. Ti/S-1, which was obtained by impregnation method, showed a huge peak near 313 nm with tiny peak at 213 nm, and for TiO_2, only an obvious peak at 313 nm was found. The absence of the band above 300 nm for TS-1b and TS-1c indicated that all of the titanium had incorporated into the framework. The results of deconvolution were shown in Fig. 5(A). The percentages of the two peaks were calculated and shown in Fig. 5(B) to show the ratio of the area of deconvoluted peaks corresponding to framework and extra-framework Ti species. It was indicated that when the Ti content was less than 1.36 wt% (Table 2), all titanium formed framework titanium species. When the titanium content exceeded this value, the excess titania would generate extra-framework titanium and the amount of extra-framework titanium species increased with increasing titanium content. That is to say, extra-framework Ti species had been generated for TS-1d and TS-1e. The results were consistent with those reported by Millini et al. [57], where the insertion of increasing amount of

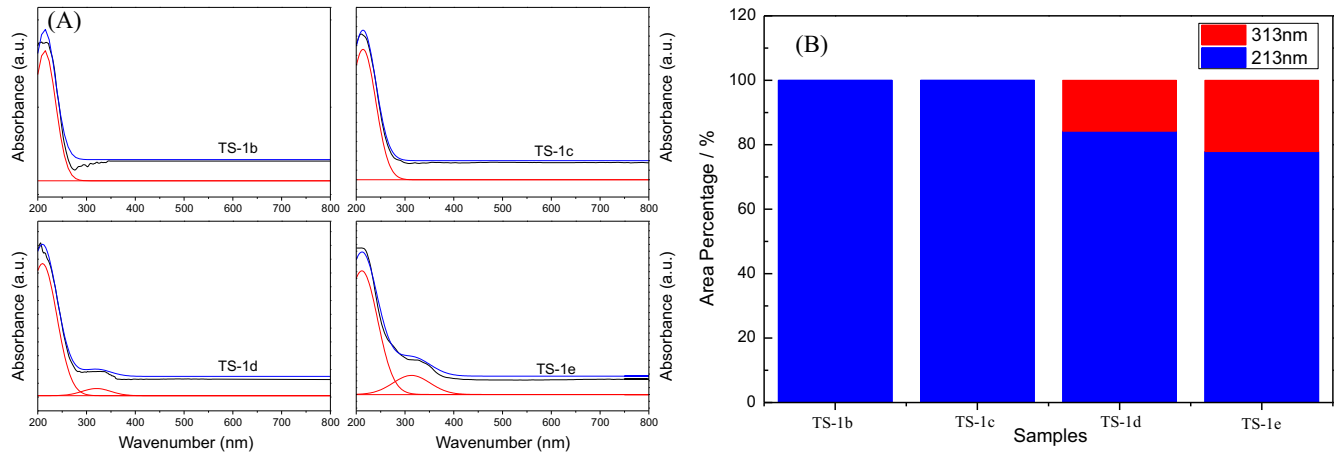

Fig. 5. (A) DR UV–vis spectra of TS-1 samples with different Ti content after deconvolution; (B) Their corresponding quantified area ratio between framework and extra-framework Ti.

Ti in the MFI framework produced a linear variation of the unit cell up to a concentration of Ti equal to 2.5 mol %, while the excess Ti segregated as extra-framework TiO_2 species.

3.1.5. XPS

The XPS results of the Ti $2p_{3/2}$ peak were shown in Fig. 6. It can be seen that only the peak at 460.0 eV was observed for TS-1b and TS-1c, which was assigned to framework Ti species [26,30]. While for TS-1d and TS-1e, besides the peak above, a new peak at 457.5 eV was found, which was assigned to extra-framework Ti [64,65]. The corresponding ratios of each species were illustrated in Table 2. It was indicated that all of the Ti species in TS-1b and TS-1c were in the framework with tetrahedral structure. In contrast, the additional extra-framework Ti was observed in TS-1d and TS-1e, and increasing Ti content would lead to an increase in the percentage of the extra-framework Ti. Overall, both UV–vis and XPS results showed that with the introduction of Ti, it incorporated into the framework firstly (TS-1a to TS-1c) with low loading, and when the critical value of 1.36 wt% for total Ti content was reached, the excess titanium generated extra framework TiO_2 species (TS-1d to TS-1e). This threshold is higher than that in some of the literatures [20,26,66], which might be caused by different preparation method used. In short, in our work, the TS-1c, TS-1d and TS-1e actually contained almost the same amount of framework titanium content, while the TS-1d and TS-1e samples also had extra-framework titanium species.

3.1.6. TEM

To further study the structure of the catalysts, the TS-1 samples with different Ti content were characterized by TEM technique, and the results were shown in Fig. 7. It was shown that the TS-1a and TS-1b exhibited similar defined cube-like morphologies with uniform size distributions. With the increase of Ti content, the cube-shaped particles gradually decreased and replaced by increasing oval grain gradually, which might be constituted by agglomerate of smaller particles [67]. When the titanium content exceeded 1.36 wt% (TS-1d and TS-1e), the petal morphology was observed. What is more, it could be found that the samples with titanium content below 2.75 wt% (TS-1a, b, c, d) showed approximately the same crystals sizes of 100 nm roughly, while the crystal diameter continued to increase to about 200 nm for TS-1e.

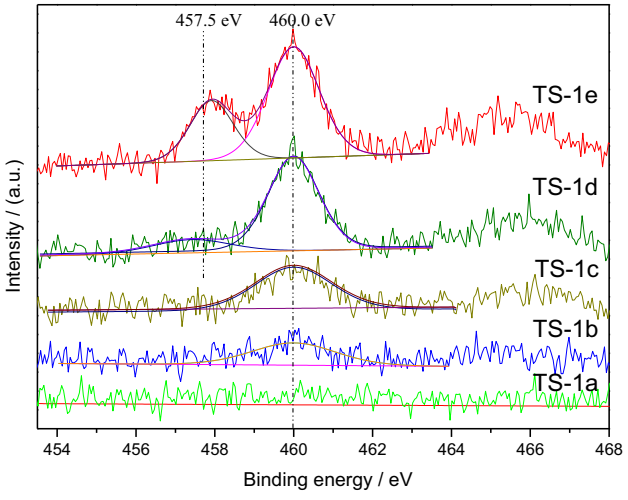

Fig. 6. The XPS results of Ti $2p_{3/2}$ spectra in TS-1 samples.

3.2. Catalytic activity

3.2.1. The influence of Ti content on the activity

In the partial oxidation of toluene, the main products were cresols, and the by-products were benzyl alcohol, benzoic acid, and methyl-p-benzoquinone. Among them, cresols and BM was the ring C—H bond activation and the side chain oxidation products respectively. MQ and HA corresponded to the further deep oxidation products of cresols and BM respectively. The catalytic activities of TS-1 with different Ti content and commercially available titanium dioxide were shown in Table 3. The conversion of toluene firstly increased with the increase of titanium content, and then remained almost unchanged around 39%. The yield of cresols increased from 8.7% (TS-1a) to 32.8% (TS-1c) firstly, and then decreased to 22.3% (TS-1e) with increasing titanium loading. The selectivity of the cresols showed the same tendency with the yield and the maximum selectivity was 84.3% obtained on TS-1c. The TOF was remained stable basically with low titanium content, and then monotonically decreased with the increasing Ti loading, where the optimal TOF was 2.66 h^{-1} obtained on TS-1c, corresponding to the highest cresols yield and selectivity. This might be due to the fact that different titanium species had different contributions to the activation of the ring and side chain C—H bonds. That is, the framework titanium species might be responsible for the hydroxylation of toluene to cresols by Ti—OOH intermediate [31]. The increased titanium content from TS-1a to TS-1c led to increased framework active centers, resulting in the higher yield of cresols. Then the excessive titanium produced extra-framework titanium species which was unfavorable for the ring C—H bond activation resulting in the reduced cresols yield for TS-1d and TS-1e. Three possibilities existed, that is, the promoted decomposition of H_2O_2 (Supplementary material, Fig. S1), side chain oxidation and further deep oxidation of the cresols and side chain oxidation products [33]. It could be observed that, the conversion of toluene kept almost the same, while the selectivity of cresols reduced significantly with the increase of extra-framework Ti species, and the yield of side chain oxidation product (BM and HA) increased obviously, indicating that the extra-framework Ti was advantageous to the oxidation of side chain under the conditions investigated in the present work. Furthermore, as shown in Table 3, the ratio of deep oxidation products, that is, HA and MQ on TS-1d and TS-1e increased, indicating the deep oxidation of both the products from the first step. To further support this view, commercially available titanium dioxide had also been used for this reaction, and 2% yield of side chain oxidation products were observed due to the absence of framework Ti species nor proper pore structure. The catalytic performance of Ti/S-1 was also comparatively studied. The conversion of toluene was only 3.7% with the 1.8% yield to side-chain products, and 1.7% ring oxidation products with the lower cresols selectivity of 35.1% was obtained for Ti/S-1. The fact that the additional Ti did not result in enhancement of conversion of toluene on Ti/S-1 might be due to its small micropore, which might have a significant impact on catalytic performance for toluene oxidation. Additionally, since Ti/S-1 was prepared by impregnation, the amount of Ti species entered into the framework of S-1 might be limited, while most of Ti species existed in extra-framework as revealed by DR UV–vis, which might be the reason of low selectivity to cresols. In addition, TS-1c demonstrated the highest catalytic performance, due to the largest BET surface and most framework Ti species with no extra-framework Ti species. The reason might be that the bigger S_{BET} was beneficial to the mass diffusion of regent together with products, and can increase the utilization of active sites.

Supplementary data associated with this article can be found, in the online version, at https://doi.org/10.1016/j.jcat.2018.07.038.

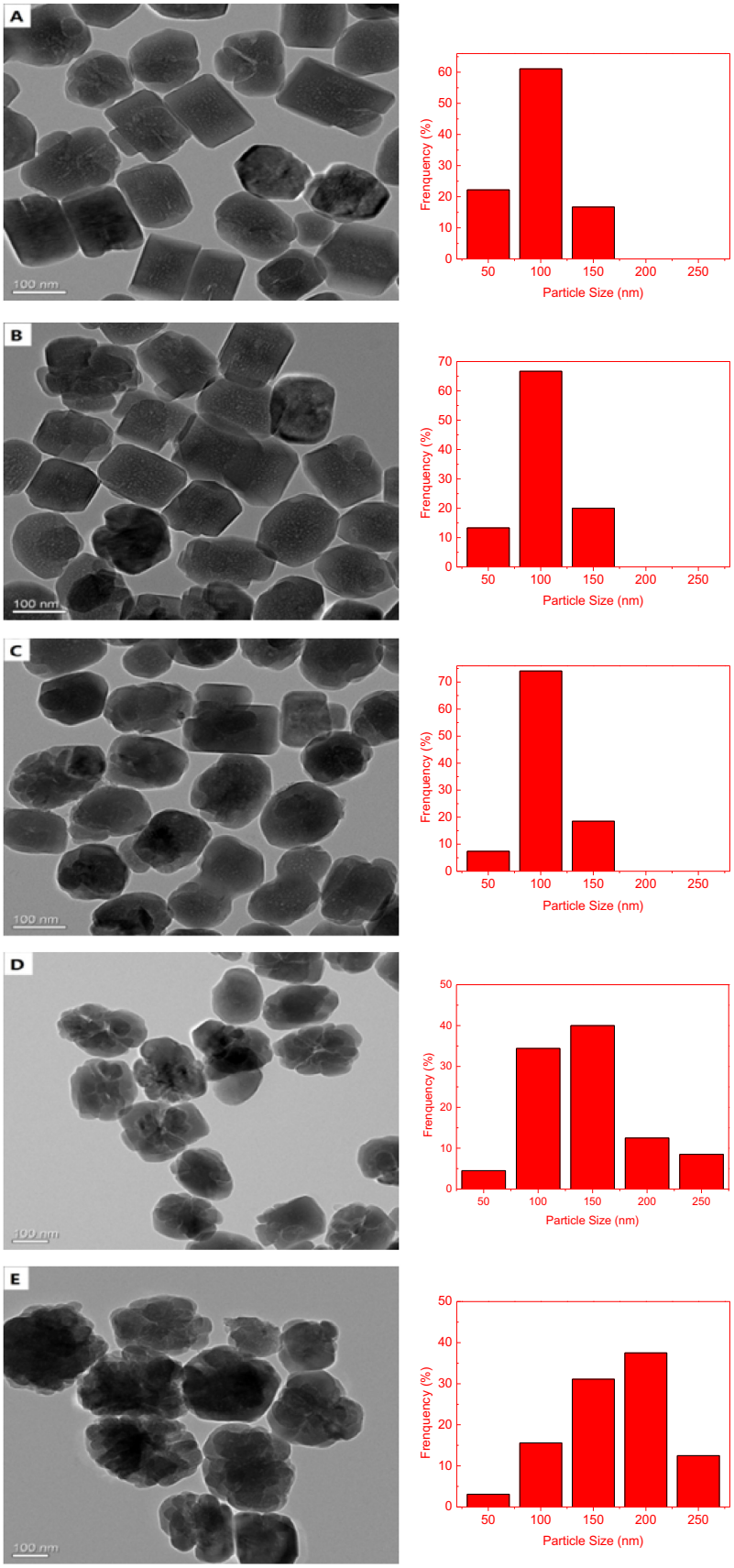

Fig. 7. TEM of TS-1 samples with different Ti content: (A) TS-1a; (B) TS-1b; (C) TS-1c; (D) TS-1d; (E) TS-1e.

Table 3
The effect of Ti content on the catalytic hydroxylation of toluene [a].

Sample	Yield (mol%)					$C_{toluene}$ (%)	$Y_{cresols}$ (%)	$S_{cresols}$ (%)	$C_{H_2O_2}$ (%)[d]	$S_{H_2O_2}$ (%)	TOF (h^{-1})
	o-cresol	p-cresol	BM[c]	HA[c]	MQ[c]						
TS-1a	1.5(12.7)[b]	7.2(61.0)	0.6	0.6	1.9	11.8	8.7	73.7	7.9	12.5	–
TS-1b	4.0(16.7)	15.8(65.8)	3.1	0.3	0.8	24.0	19.8	82.5	5.1	30.1	2.62
TS-1c	6.8(17.4)	26.0(66.8)	4.7	0.7	0.7	38.9	32.8	84.3	5.5	44.5	2.66
TS-1d	6.2(15.8)	22.7(57.8)	8.5	0.7	1.2	39.3	28.9	73.5	9.3	27.2	1.16
TS-1e	4.5(12.0)	17.8(47.5)	11.4	1.5	2.3	37.5	22.3	59.5	13.2	20.0	0.44
TiO_2	–	–	0.2	–	–	0.2	–	–	13.6	0.1	–
Ti/S-1	0.8(21.6)	0.5(16.1)	1.6	0.2	0.6	3.7	1.3	35.1	9.0	3.5	0.03

[a] Reaction conditions: 0.5 g catalyst, 2.3 mmol toluene, 39.2 mmol H_2O_2, 30 mL H_2O, 60 °C, 120 min.
[b] The values in parentheses were the corresponding selectivity of o-cresol and p-cresol.
[c] BM, HA, MQ represented benzyl alcohol, benzoic acid and methyl-p-benzoquinone, respectively.
[d] Remained amount of H_2O_2 was determined by indirect iodimetry under acidic condition.

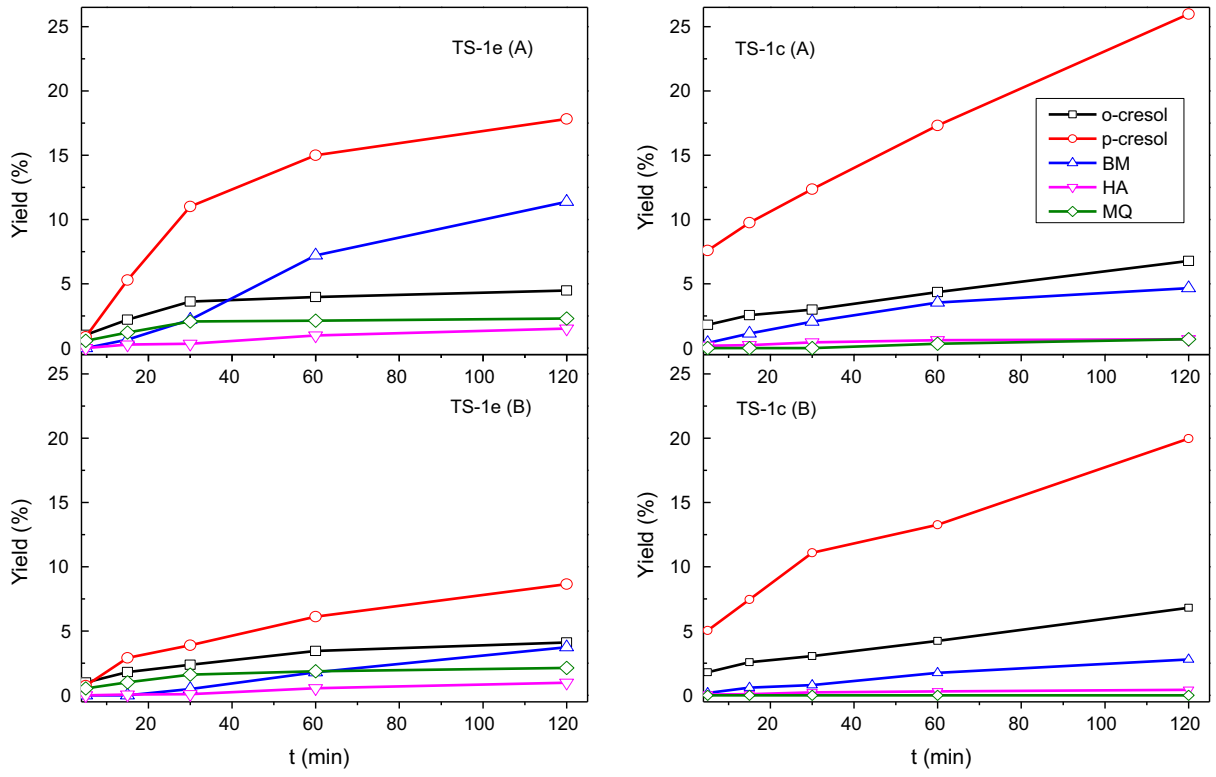

Fig. 8. Plots of products yield from toluene over TS-1c and TS-1e. (A) In the absence of isopropanol; (B) In the presence of isopropanol (2.6 mmol).

As described in related literatures, framework Ti in TS-1 interacted with hydrogen peroxide giving rise to the formation of a Ti—OOH species that could perform selective oxidation of hydrocarbons through an non-radical mechanism [68], while the extra-framework Ti could promote extensive homolytic side reaction including decomposition of hydrogen peroxide, which followed a free-radical mechanism [57]. In order to clarify the reaction mechanism of toluene partial oxidation, the influence of isopropanol, a known hydroxyl radical (·OH) scavenger [69], on the performance of TS-1c and TS-1d was examined. The results were shown in Fig. 8. It was indicated that hydroxyl radical species might play a significant role in side-chain oxidation. Compared with the reactions catalyzed by these two different kinds of TS-1 samples, TS-1e was significantly affected by isopropanol, while TS-1c was not very obvious. Detection of free radical was also carried by EPR to further confirm the role of radical species in TS-1/H_2O_2/H_2O/toluene system. The reaction was performed under the conditions of 0.5 g TS-1c or TS-1e catalysts, 2.3 mmol toluene, 39.2 mmol H_2O_2, 30 mL H_2O at room temperature. After 30 min, we pipetted

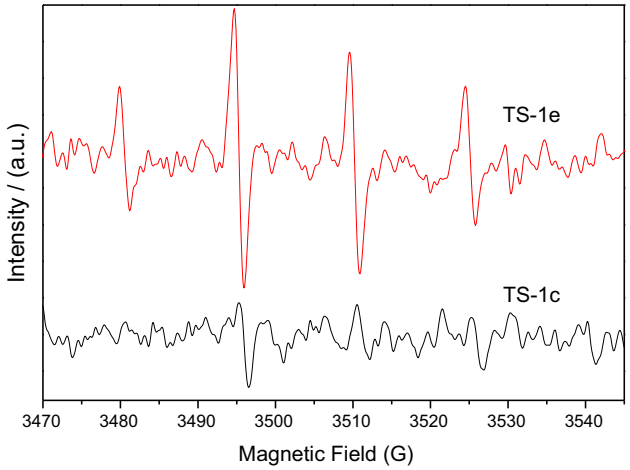

Fig. 9. The EPR spectra of DMPO spin-trapping.

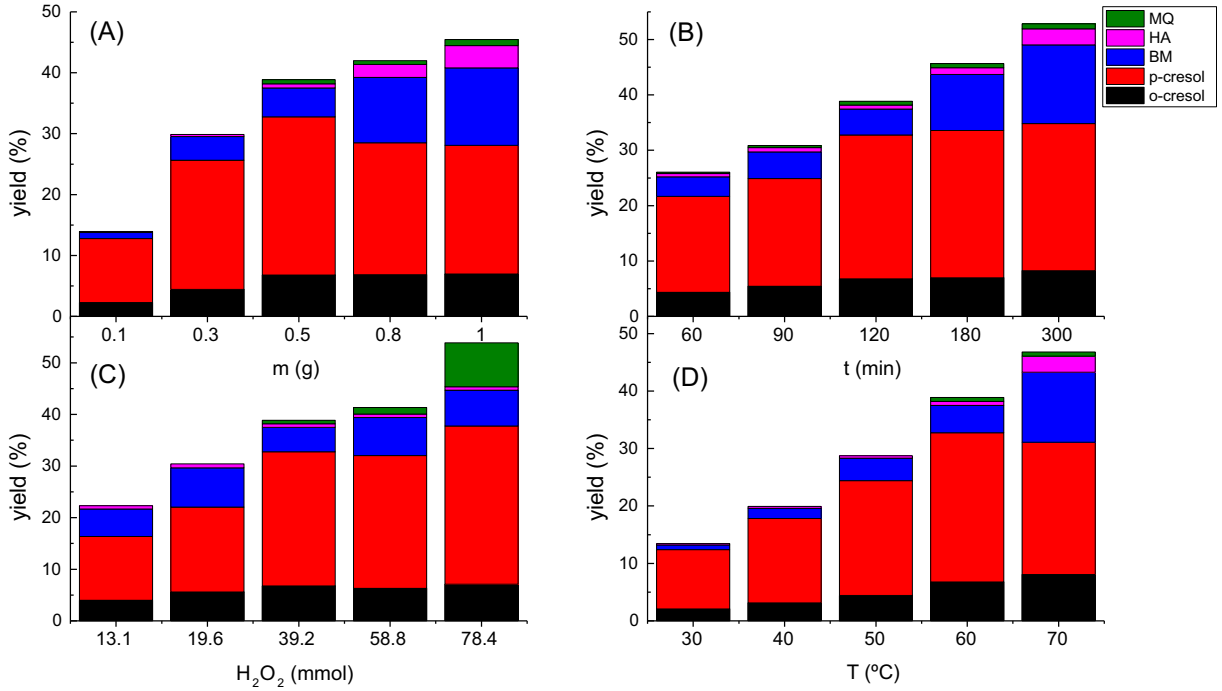

Fig. 10. Optimization of reaction parameters: (A) The influence of the amount of TS-1c; (B) The influence of reaction time; (C) The influence of the H_2O_2 dosage; (D) The influence of temperature.

0.1 mL the supernatant liquid and added 0.02 mL 5, 5-Dimethyl-pyrroline-oxide (DMPO). The results were shown in Fig. 9. Clearly, a quartet of signals with relative intensities of 1:2:2:1 from the DMPO-OH· adducts were detected during the reaction process at room temperature catalyzed by TS-1e, suggesting the presence of homolysis of H_2O_2. However, this phenomenon was not observed for the system catalyzed by TS-1c, with absence of extra-framework Ti species. It appears clear that in toluene oxidation with TS-1 and hydrogen peroxide the ring hydroxylation was catalyzed by framework titanium-hydroperoxo sites which could not be detected by DMPO spin-trapping, while the side chain oxidation occurred through a radical mechanism promoted by extra-framework Ti.

Titanium effect was also observed in benzene hydroxylation, Barbera et al. [4] found that the framework Ti species led to the formation of Ti sites in tetrahedral coordination and Ti—OOH was the active intermediate which was responsible for hydroxylation of benzene to phenol. Similarly, the different Ti species was also considered to play different roles in propylene epoxidation. Xiong et al. [20] also proposed that Ti—OOH was the active intermediate for propylene epoxidation, and they thought that the acid sites generated by extra-framework species led to further oxidization of the propylene oxide. Thus, over the catalysts (TS-1d and TS-1e) with higher extra-framework Ti species, the deep oxidation was also more obvious. Combining the literatures above, we thought that the partial oxidation of toluene was proceeded according to the following mechanism. Firstly, the framework Ti was responsible for the ring C—H bond activation to produce cresols by framework Ti-hydroperoxo sites, while the side chain oxidation products (benzyl alcohol) occurred though a radical mechanism promoted by extra-framework Ti species. Then, the further deep oxidation of both ring C—H activation products and side chain oxidation products further proceeded, that is, the cresols were further oxidized to methyl-p-benzoquinone, and the benzyl alcohol was further oxidized to benzoic acid by extra-framework Ti.

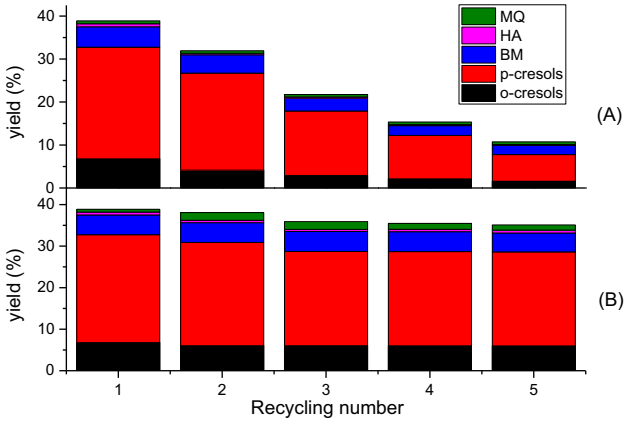

Fig. 11. Activity test of the used catalyst: (A) The used catalysts were only dried; (B) The used catalysts were dried and calcined.

3.2.2. Optimization of reaction parameters[1]

According to the above results obtained, TS-1c was selected to optimize the reaction conditions, where the effect of the amount of TS-1c, the reaction temperature, the amount of H_2O_2 and the reaction time on the reaction was optimized. The results were shown in Fig. 10. As could be seen, the highest yield of 32.8% to cresols was obtained with the selectivity of 84.3%, under the optimized conditions of 0.5 g TS-1c, 2.3 mmol toluene, 39.2 mmol H_2O_2, 30 mL H_2O, in 60 °C water-bath for 120 min. The stability of the final observed products under the reactions was good, especially o-cresol, BM, HA and MQ (Supplementary material, Fig. S2). Moreover, this reaction was clearly observed to show a high

[1] Reaction condition: (A) 2.3 mmol toluene, 39.2 mmol H_2O_2, 30 mL H_2O, 60 °C, 120 min; (B) 0.5 g TS-1c, 2.3 mmol toluene, 39.2 mmol H_2O_2, 30 mL H_2O, 60 °C; (C) 0.5 g TS-1c, 2.3 mmol toluene, V_{H2O}:V_{H2O2} = 15:2, 60 °C; 120 min; (D) 0.5 g TS-1c, 2.3 mmol toluene, 39.2 mmol H_2O_2, 30 mL H_2O, 120 min.

selectivity to para-isomer, which was considered to be characteristic for process *via* electrophilic mechanism, being consistent with the results in Ref [35,70]. Combining with steric hindrance of methyl in toluene, the substrate was superior to the para-position [14]. In addition, it was clear that the TS-1 catalysts prepared by modified hydrothermal synthesis method exhibited obvious para-selectivity, while the Ti/S-1 obtained by impregnation method showed the ortho-priority. This could be explained by the pore size distribution. Obviously, the TS-1 samples had a smaller average pore size of 19.62–27.29 Å, while the Ti/S-1 samples showed the average pore size of 31.79 Å. In summary, the size of para-position product might be more accessible to the smaller channel and be in touch with the active titanium center in TS-1 samples. However, the ortho-hydroxylation occurred in the bigger pores of Ti/S-1 samples. Furthermore, it was observed that the products with larger molecular size, such as o-cresols (5.71 Å) and methyl-p-benzoquinone (5.64 Å), were easier to generate in larger pores. However, since the molecular dimensions of other products were only 4.32 Å, it was dominant in smaller pores.

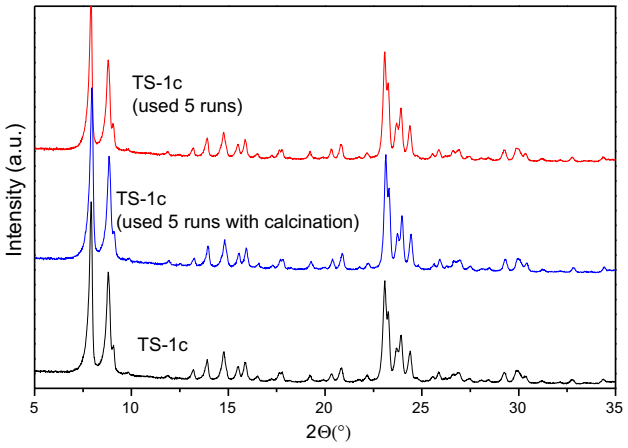

Fig. 12. XRD patterns of fresh and deactivated TS-1c sample.

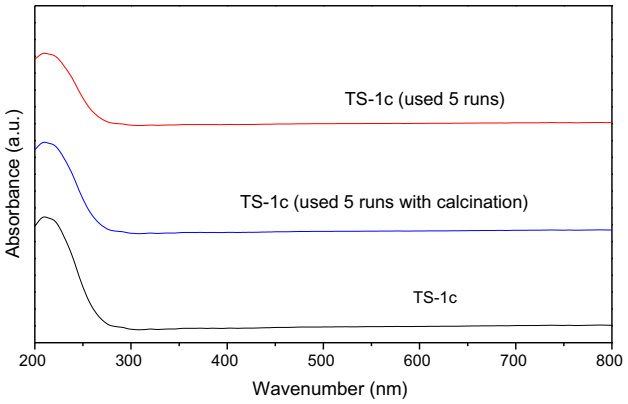

Fig. 13. DR UV–vis patterns of fresh and deactivated TS-1c sample.

3.3. Recycle of the catalysts

The spent catalysts were reused to test the stability of the catalysts. As can be seen in Fig. 11, when the used catalysts were only dried at 100 °C overnight, both the conversion of toluene and the yield of cresols showed a monotonic decreasing trend. However, if the used catalysts were dried overnight and calcined at 550 °C for 10 h, the conversion and yield remained essentially stable after being reused for two runs, and 28.6% yield and 81.5% selectivity to cresols were obtained under the optimal conditions with 0.5 g TS-1c used for 5 runs. According to related reports in the literatures [23,32,71], the deactivation of TS-1 was likely to be attributed to following three reasons: dissolution of Ti species, migration of Ti species and organic by-products filling in the micropores of TS-1 zeolite. The two former reasons caused irreversible deactivation [30,32], while the latter could be regenerated by calcination or washing with dilute hydrogen peroxide [72]. Firstly, based on XRD (Fig. 12), no significant differences were observed when TS-1c was used repeatedly for 5 times, indicating the fresh TS-1c and deactivated sample had almost the same crystal and the excellent MFI topological structure. Similarly, the catalysts were characterized by DR UV–vis (Fig. 13) and XPS (Fig. 14), and both fresh and deactivated catalysts showed the same Ti $2p_{3/2}$ spectra, demonstrating that the titanium species did not migrate [32]. However, the spectra of C 1s showed obvious changes, for a new band at 285.5 eV appeared in the deactivated TS-1c, in addition to the graphltic carbon groups on every samples (peak at 284.5 eV), indicating that the carbon presented in alcohol, phenolic and ether groups [33]. This might be caused by fouling by deposition of heavy by-products. The surface area and pore volumes of these samples were summarized in Table 4. It could be seen that the specific surface area and the micropore volumes decreased gradually with the increase of reuse times, indicating the channels of the spent TS-1 catalysts were blocked by the above species. Supplementary as shown in Fig. 18, if the deactivated TS-1c sample (used 5 runs) was calcined at 550 °C, the S_{BET} and V_{mic} could be restored, which was consistent with the literature [32,72].

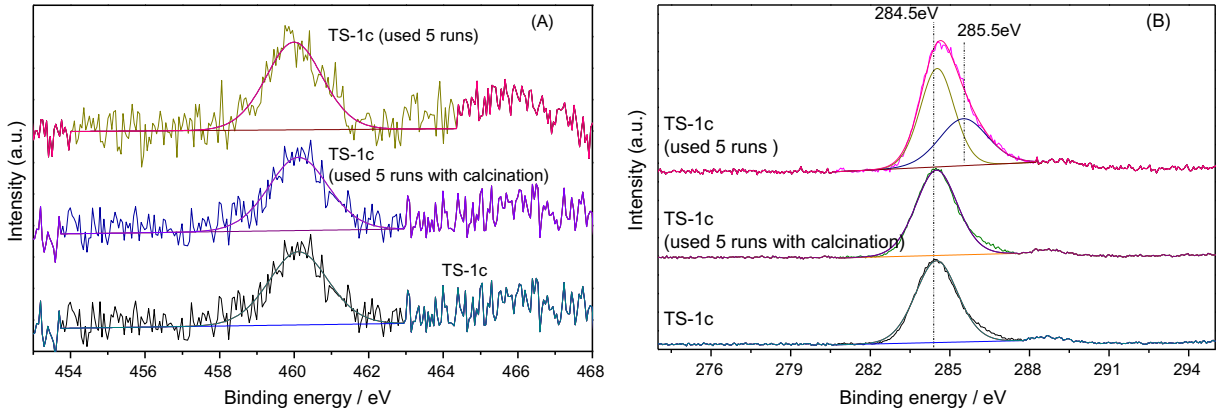

Fig. 14. The XPS patterns of fresh and deactivated TS-1c samples: (A) Ti $2p_{3/2}$ spectra of the samples; (B) C 1 s spectra of the samples.

Table 4
The Physical property for fresh and used TS-1c samples.

Sample	S_{BET} (m^2/g)	V_{total} (cm^3/g)	V_{mic} (cm^3/g)	V_{meso} (cm^3/g)	D_{avg} (Å)	TG[a] (wt%)	EDS[b] (wt%)	ICP[c] (wt%)
TS-1c	463.54	0.34	0.16	0.18	23.11	0.75	–	1.36
TS-1c (used once)	303.80	0.28	0.12	0.16	25.02	4.06	7.46	1.33
TS-1c (used 2 runs)	291.04	0.30	0.10	0.20	28.42	5.92	7.63	1.31
TS-1c (used 3 runs)	286.49	0.28	0.09	0.19	25.67	6.35	8.67	1.31
TS-1c (used 4 runs)	247.21	0.29	0.10	0.19	29.04	6.77	9.08	1.31
TS-1c (used 5 runs)	253.65	0.29	0.10	0.19	28.20	6.97	15.47	1.31
TS-1c (used 5 runs with calcination)	445.04	0.34	0.17	0.17	24.15	1.66	–	1.31

[a] The weight loss rate of the samples in TG analysis.
[b] The carbon content of the spent TS-1c samples measured by SEM-EDS.
[c] The titanium content analyzed by ICP-AES.

To confirm the cause of catalyst deactivation by carbon deposition, TG-DTG curves (Fig. 15) of the fresh and used TS-1 were carried out. It was seen that the weight loss was increased with the used times (Table 4). Nevertheless, the calcined used TS-1c was similar to fresh one for almost no weight loss, which indicated an easily firing species was formed over the deactivated catalyst. TG-DTG curves of the fresh TS-1 catalysts were similar to the regenerated one, which only had one stage of weight loss over the low temperature range of about 100–200 °C. However, there were two distinct stages in the deactivated catalysts, the first stage of weight loss at the range of 100–250 °C was attributed to desorption of H_2O and the organic by-products on the catalyst surface, and the other at the range of 300–600 °C was attributed to the oligomeric compounds inside the channel of the catalyst [72,73].

In order to investigate the species of the deposition on the deactivated catalysts, the TS-1c (used 5 runs) was characterized by *in situ* FT-IR, and the results were shown in Fig. 16. With increasing temperature in dry air, obvious reduction had been observed for the following peaks: the band at 3000 and 1680 cm^{-1} attributed to aromatic C=C stretching vibration [74], the peak at 1370 cm^{-1} to methyl (CH_3), the bands over the range of 3600–3100 cm^{-1} and at 1200 cm^{-1} to the stretching vibration of O—H bond [75], the bands at 1900–1680 cm^{-1} to C=O, and the region of 1850 cm^{-1} and 1740 cm^{-1} summarized as acid anhydride. These changes might be caused by the removal of polymer species which were adsorbed in the pores. This result was coincident with the TG-DTG curves above.

Fig. 17 showed the EDS analysis of the used TS-1, and the carbon content was listed in Table 4. It indicated that with the increasing of used times, higher carbon content has been found.

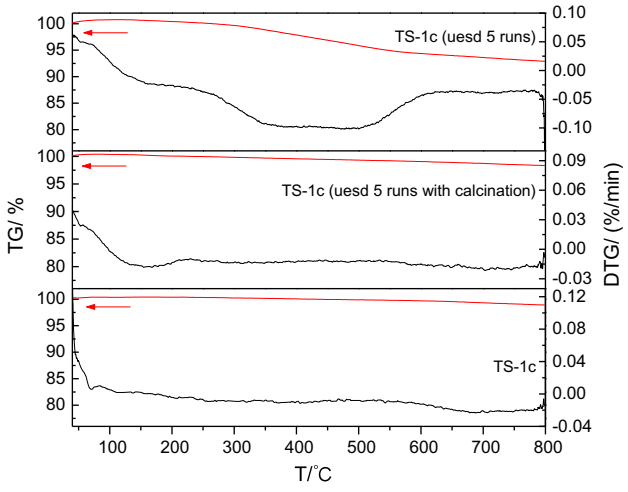

Fig. 15. The TG-DTG characterization of the used TS-1 samples.

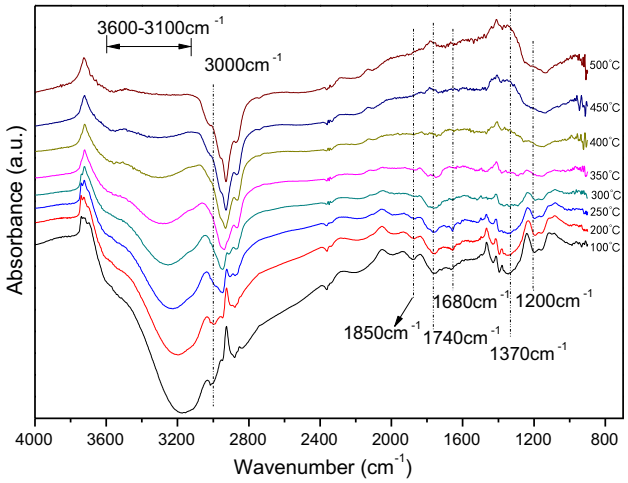

Fig. 16. The *in situ* FT-IR spectra of the deactivated TS-1c sample.

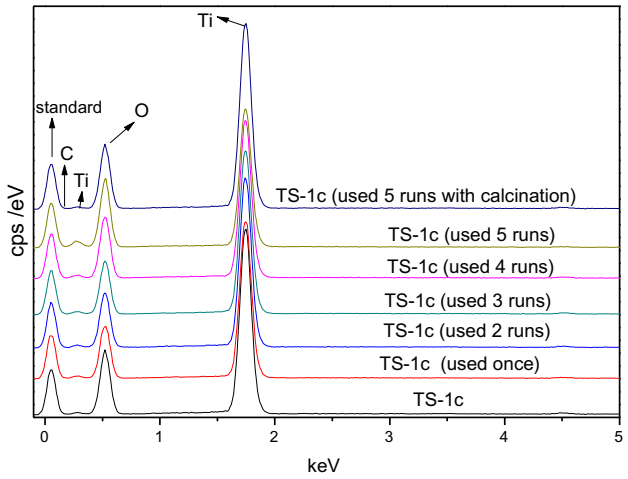

Fig. 17. The SEM-EDS analyses of used TS-1 samples.

All of these evidences showed that the deactivation was caused by carbon deposition. Interestingly, the catalyst performance of the calcined catalyst was not recovered completely during the first two repeated runs. To explore the reason, the filtrate after reaction was analyzed by ICP characterization, and the amounts of leached Ti in the first two runs were 2.2 wt% and 1.5 wt% respectively. That is, leaching of the framework titanium also contributed to the deactivation of the TS-1 samples for the first two runs, which was irreversible. After two runs, the catalyst became stable.

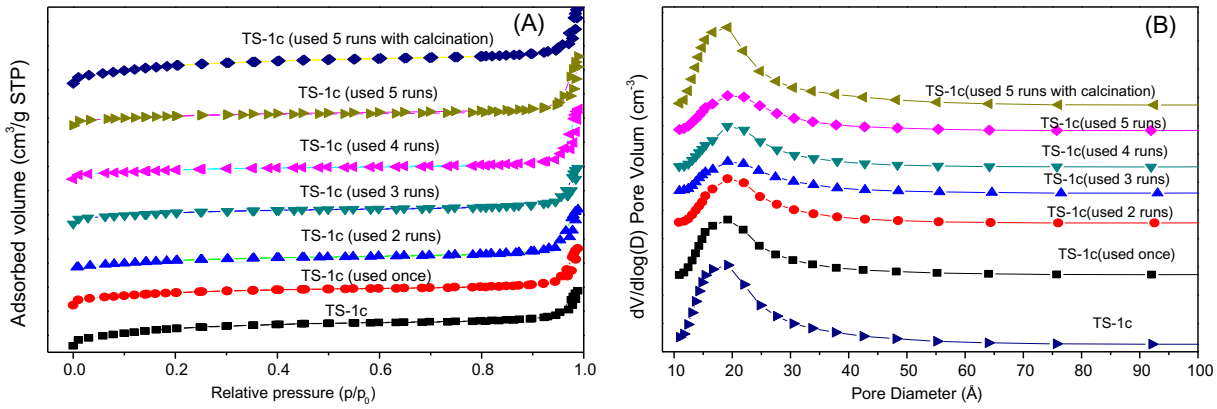

Fig. 18. (A) N_2 adsorption-desorption isotherms of the used TS-1; (B) The pore diameter distribution of the used TS-1 catalysts.

4. Conclusions

In conclusion, the threshold of Ti to incorporate into the Si framework was 1.36 wt% by a modified hydrothermal synthesis method used in the present work. The two kinds of Ti species on TS-1 had different contributions to the partial oxidation of toluene, that is, the framework Ti was responsible for the ring C—H bond activation to produce cresols, while the extra-framework Ti was advantageous to the formation of side chain oxidation products and to the deep oxidation of both kinds of the products formed in the first step. In toluene oxidation with TS-1 and hydrogen peroxide the ring hydroxylation was performed by framework titanium-hydroperoxo sites, while the side chain oxidation occurred through a radical mechanism promoted by extra-framework Ti. The highest yield of 32.8% to cresols was obtained with the selectivity of 84.3%, under the optimized reaction condition of 0.5 g TS-1c, 2.3 mmol toluene, 39.2 mmol H_2O_2, 30 mL H_2O, in 60 °C water-bath for 120 min. Para-cresol was produced with high selectivity (66.8%), which might be caused by the pore structure of the catalyst and steric hindering of methyl group. The catalyst could be regenerated by calcination, and the regenerated catalyst exhibited stable activity and selectivity after the second run.

Acknowledgement

The authors gratefully acknowledged the financial supports from NSFC (No. 21372167 No. 21172157) as well as the province from Sichuan (2016JY0181) and the province supported by the Fundamental Research Funds for the Central Universities (SCU2018D003, SCU2017D007). The technical support was provided by Analytical and Testing Center of Sichuan University. Especially, we would like to thank Yuefei Tian of the Analytical and Testing Center of Sichuan University for the XPS characterization.

References

[1] N.A. Romero, K.A. Margrey, N.E. Tay, D.A. Nicewicz, Science 349 (2015) 1326–1330.
[2] Q. Liu, L. Zhu, L. Li, B. Guo, X. Hu, C. Hu, J. Mol. Catal. A: Chem. 331 (2010) 71–77.
[3] Y. Luo, J. Xiong, C. Pang, G. Li, C. Hu, Catalysts 8 (2018) 49.
[4] D. Barbera, F. Cavani, T. D'Alessandro, G. Fornasari, S. Guidetti, A. Aloise, G. Giordano, M. Piumetti, B. Bonelli, C. Zanzottera, J. Catal. 275 (2010) 158–169.
[5] M. Feller, A. Karton, G. Leitus, J.M.L. Martin, D. Milstein, J. Am. Chem. Soc. 128 (2006) 12400–12401.
[6] D. Wang, X. Yu, X. Xu, B. Ge, X. Wang, Y. Zhang, Chem. Eur. J. 22 (2016) 8663–8668.
[7] S. Bag, R. Jayarajan, R. Mondal, D. Maiti, Angew. Chem. Int. Ed. 56 (2017) 3182–3186.
[8] C.W. Yoon, K.F. Hirsekorn, M.L. Neidig, X. Yang, T.D. Tilley, ACS Catal. 1 (2011) 1665–1678.
[9] G. Bellussi, R. Millini, P. Pollesel, C. Perego, New J. Chem. 40 (2016) 4061–4077.
[10] C. Perego, R. Millini, Chem. Soc. Rev. 42 (2013) 3956–3976.
[11] W. Fan, R.-G. Duan, T. Yokoi, P. Wu, Y. Kubota, T. Tatsumi, J. Am. Chem. Soc. 130 (2008) 10150–10164.
[12] T. Yu, Q. Zhang, S. Xia, G. Li, C. Hu, Catal. Sci. Technol. 4 (2014) 639–647.
[13] B. Guo, Q. Zhang, G. Li, J. Yao, C. Hu, Green Chem. 14 (2012) 1880.
[14] C. Xia, L. Long, B. Zhu, M. Lin, X. Shu, Catal. Commun. 80 (2016) 49–52.
[15] X. Wang, Y. Guo, X. Zhang, Y. Wang, H. Liu, J. Wang, J. Qiu, K.L. Yeung, Catal. Today 156 (2010) 288–294.
[16] S.-T. Tsai, P.-Y. Chao, T.-C. Tsai, I. Wang, X. Liu, X.-W. Guo, Catal. Today 148 (2009) 174–178.
[17] X. Wang, X. Zhang, Y. Wang, H. Liu, J. Qiu, J. Wang, W. Han, K.L. Yeung, Chem. Mater. 23 (2011) 4469–4479.
[18] S. Xia, T. Yu, H. Liu, G. Li, C. Hu, Catal. Sci. Technol. 4 (2014) 3108–3119.
[19] M. Liu, H. Wei, B. Li, L. Song, S. Zhao, C. Niu, C. Jia, X. Wang, Y. Wen, Chem. Eng. J. 331 (2018) 194–202.
[20] G. Xiong, Y. Cao, Z. Guo, Q. Jia, F. Tian, L. Liu, Phys. Chem. Chem. Phys. 18 (2016) 190–196.
[21] W.-S. Lee, M. Cem Akatay, E.A. Stach, F.H. Ribeiro, W. Nicholas Delgass, J. Catal. 287 (2012) 178–189.
[22] L. Wang, G. Xiong, J. Su, P. Li, H. Guo, J. Phys. Chem. C 116 (2012) 9122–9131.
[23] Y. Wang, S. Zhang, Y. Zhao, M. Lin, J. Mol. Catal. A: Chem. 385 (2014) 1–6.
[24] A. Zheng, C. Xia, Y. Xiang, M. Xin, B. Zhu, M. Lin, G. Xu, X. Shu, Catal. Commun. 45 (2014) 34–38.
[25] X. Wang, X. Zhang, Y. Wang, H. Liu, J. Qiu, J. Wang, W. Han, K.L. Yeung, ACS Catal. 1 (2011) 437–445.
[26] G. Zou, W. Zhong, L. Mao, Q. Xu, J. Xiao, D. Yin, Z. Xiao, S.R. Kirk, T. Shu, Green Chem. 17 (2015) 1884–1892.
[27] X. Lu, Y. Guan, H. Xu, H. Wu, P. Wu, Green Chem. 19 (2017) 4871–4878.
[28] N. Wilde, M. Pelz, S.G. Gebhardt, R. Gläser, Green Chem. 17 (2015) 3378–3389.
[29] R. Millini, G. Perego, K. Seiti, Stud. Surf. Sci. Catal. 84 (1994) 2123–2129.
[30] A.C. Alba-Rubio, J.L.G. Fierro, L. León-Reina, R. Mariscal, J.A. Dumesic, M. López Granados, Appl. Catal. B 202 (2017) 269–280.
[31] X. Feng, N. Sheng, Y. Liu, X. Chen, D. Chen, C. Yang, X. Zhou, ACS Catal. 7 (2017) 2668–2675.
[32] C. Xia, M. Lin, A. Zheng, Y. Xiang, B. Zhu, G. Xu, X. Shu, J. Catal. 338 (2016) 340–348.
[33] H. Liu, G. Li, C. Hu, J. Mol. Catal. A: Chem. 377 (2013) 143–153.
[34] Y. Zhong, G. Li, L. Zhu, Y. Yan, G. Wu, C. Hu, J. Mol. Catal. A: Chem. 272 (2007) 169–173.
[35] D. Zhang, L. Gao, Y. Wang, W. Xue, X. Zhao, S. Wang, Catal. Commun. 12 (2011) 1109–1112.
[36] A. Raba, M. Cokoja, W.A. Herrmann, F.E. Kuhn, Chem Commun. 50 (2014) 11454–11457.
[37] X. Liu, C. Yang, Y. Wang, Y. Guo, Y. Guo, G. Lu, Chem. Eng. J. 243 (2014) 192–196.
[38] V.A. de la Pena O'Shea, M. Capel-Sanchez, G. Blanco-Brieva, J.M. Campos-Martin, J.L. Fierro, Angew. Chem. Int. Ed. 42 (2003) 5851–5854.
[39] K. Bendahou, L. Cherif, S. Siffert, H.L. Tidahy, H. Benaïssa, A. Aboukaïs, Appl. Catal. A 351 (2008) 82–87.
[40] Z. Qu, Y. Bu, Y. Qin, Y. Wang, Q. Fu, Chem. Eng. J. 209 (2012) 163–169.
[41] W. Zhong, S.R. Kirk, D. Yin, Y. Li, R. Zou, L. Mao, G. Zou, Chem. Eng. J. 280 (2015) 737–747.
[42] B. Du, S.-I. Kim, L.-L. Lou, A. Jia, G. Liu, B. Qi, S. Liu, Appl. Catal. A 425–426 (2012) 191–198.
[43] X. Li, B. Lu, J. Sun, X. Wang, J. Zhao, Q. Cai, Catal. Commun. 39 (2013) 115–118.
[44] B. Puértolas, L. García-Andújar, T. García, M.V. Navarro, S. Mitchell, J. Pérez-Ramírez, Appl. Catal. B 154–155 (2014) 161–170.

[45] M. Popova, Á. Szegedi, P. Németh, N. Kostova, T. Tsoncheva, Catal. Commun. 10 (2008) 304–308.
[46] M. Popova, A. Szegedi, Z. Cherkezova-Zheleva, I. Mitov, N. Kostova, T. Tsoncheva, J. Hazard. Mater. 168 (2009) 226–232.
[47] X. Fu, Y. Liu, W. Yao, Z. Wu, Catal. Commun. 83 (2016) 22–26.
[48] Y. Zhong, G. Li, L. Zhu, D. Tang, C. Hu, J. Chinese U. 28 (2007) 1570–1572.
[49] Y. Qin, Z. Qu, C. Dong, N. Huang, Chin. J. Catal. 38 (2017) 1603–1612.
[50] B. Guo, L. Zhu, X. Hu, Q. Zhang, D. Tong, G. Li, C. Hu, Catal. Sci. Technol. 1 (2011) 1060.
[51] J.A. Martens, P. Buskens, P.A. Jacobs, Appl. Catal. A 99 (1993) 71–84.
[52] J. Li, J. Li, Z. Zhao, X. Fan, J. Liu, Y. Wei, A. Duan, Z. Xie, Q. Liu, J. Catal. 352 (2017) 361–370.
[53] G. Li, C. Zhang, Z. Wang, H. Huang, H. Peng, X. Li, Appl. Catal. A 550 (2018) 67–76.
[54] M. Du, G. Zhan, X. Yang, H. Wang, W. Lin, Y. Zhou, J. Zhu, L. Lin, J. Huang, D. Sun, L. Jia, Q. Li, J. Catal. 283 (2011) 192–201.
[55] R. Millini, G. Bellussi, Catal, Sci. Technol. 6 (2016) 2502–2527.
[56] R. Millini, G. Perego, D. Berti, W.O.P. Jr., A. Carati, G. Bellussi, Micropor. Mesopor. Mater. 35–36 (2000) 387–403.
[57] R. Millini, E.P. Massara, G. Perego, G. Bellussi, J. Catal. 137 (1992) 497–503.
[58] T. Yu, R. Yang, S. Xia, G. Li, C. Hu, Catal. Sci. Technol. 4 (2014) 3159–3167.
[59] P. Stathi, Y. Deligiannakis, M. Louloudi, Catal. Today 242 (2015) 146–152.
[60] J. Wallace, O. Parker, R. Millini, J. Am. Chem. Soc. 128 (2006) 1450–1451.
[61] L. Balducci, D. Bianchi, R. Bortolo, R. D'Aloisio, M. Ricci, R. Tassinari, R. Ungarelli, Angew. Chem. Int. Ed. 42 (2003) 4937–4940.
[62] M. Wang, J. Zhou, G. Mao, X. Zheng, Ind. Eng. Chem. Res. 51 (2012) 12730–12738.
[63] D.-G. Huang, X. Zhang, B.-H. Chen, Z.-S. Chao, Catal. Today 158 (2010) 510–514.
[64] G. Wu, J. Xiao, L. Zhang, W. Wang, Y. Hong, H. Huang, Y. Jiang, L. Li, C. Wang, RSC Adv. 6 (2016) 101071–101078.
[65] C. Liu, J. Huang, D. Sun, Y. Zhou, X. Jing, M. Du, H. Wang, Q. Li, Appl. Catal. A 459 (2013) 1–7.
[66] X. Wang, P. Zhang, X. Liu, B. Zhang, Appl. Surf. Sci. 254 (2007) 544–547.
[67] G. Bellussi, R. Millini, Struct Bond, Spring International Publishing AG, 2017.
[68] T. Lu, J. Zou, Y. Zhan, X. Yang, Y. Wen, X. Wang, L. Zhou, J. Xu, ACS Catal. (2018) 1287–1296.
[69] M. Mrowetz, E. Selli, PCCP 7 (2005) 1100.
[70] A. Costine, T. O'Sullivan, B.K. Hodnett, Catal. Today 99 (2005) 199–208.
[71] X. Zhang, Y. Wang, F. Xin, Appl. Catal. A 307 (2006) 222–230.
[72] Q. Wang, L. Wang, J. Chen, Y. Wu, Z. Mi, J. Mol. Catal. A: Chem. 273 (2007) 73–80.
[73] H. Liu, G. Lu, Y. Guo, Y. Guo, J. Wang, Chem. Eng. J. 108 (2005) 187–192.
[74] Z. Niu, G. Liu, H. Yin, D. Wu, C. Zhou, Fuel 172 (2016) 1–10.
[75] Z. Niu, G. Liu, H. Yin, C. Zhou, D. Wu, B. Yousaf, C. Wang, Energy Convers. Manage. 124 (2016) 180–188.